

2. VARIATIONS IN STRUCTURAL STYLE WITHIN PERUVIAN FOREARC SEDIMENTS¹

Alan E. S. Kemp² and Nancy Lindsley-Griffin³

ABSTRACT

The Peruvian forearc has a history of both tectonic erosion and accretion during the Neogene in the sector drilled during Leg 112. The effects of these processes are represented in the deformational features encountered in the 10 sites occupied. A wide range of environments, from shelf and upper-slope basins through mid-slope to the lower slope, were sampled. From analysis of structural features, a number of distinct tectonic provinces having characteristic structural styles can be delineated. Shelf and upper-slope basins are characterized by veins that infill *en-echelon* tension gashes, extensional microfaults, and larger discrete gashes. These features probably formed in response to the Pliocene-Quaternary extension, subsidence, and dewatering in these basins. Pliocene-Miocene slope sediments underwent locally intense fracturing at depth, which was a significant obstacle to drilling. Site 685 on the lower slope contains the clearest junction between slope cover and accretionary complex yet encountered during DSDP and ODP drilling. Upper Miocene sediments from the accretionary complex exhibit a scaly foliation and compression-related fracturing. The Pliocene-Miocene section in the lower-slope basin at Site 688 is pervasively deformed and probably represents a semicoherent submarine slide mass whose emplacement may have coincided with the passage of the Nazca Ridge across the margin. Deformation in the Eocene rocks of Sites 682 and 688, including scaly foliation, faulting, and folding, probably formed during a late Eocene/Oligocene tectonic episode.

INTRODUCTION

Offshore drilling and field studies on land have demonstrated the great diversity and complexity of structural style associated with accretionary complexes. Although penetration into active forearcs during DSDP/ODP drilling has mainly been limited to a few hundred meters, results of this (synthesized in Moore, 1986) have greatly increased our awareness of deformation in forearc regions. Increasingly, it is apparent that the structural evolution of forearcs is a complex interplay between lithology and convergence history, and that every margin drilled is distinct in many respects. Recent studies have suggested that research on active margins should be directed at processes at the thrust front, their deep structure, and fluid circulation (Moore et al., 1985; COSOD II, 1987). However, drilling results suggest that further characterization of relatively superficial levels of forearcs is still urgently required to improve our understanding of the variety of processes that may operate.

In particular, studies of modern forearcs have highlighted the wide range of "tectonic" features that can form in unconsolidated sediments. Expectations of DSDP and ODP forearc drilling have been substantial. Key aims of scientists studying modern and ancient forearc complexes include a wish for indicators of tectonic style to distinguish different tectonic environments and for criteria for distinguishing deformation of "soft" and lithified sediments. It is clear from recent studies that such criteria are elusive.

Although primarily aimed at larger-scale tectonic problems, Leg 112 drilling also shed light on the evolution and origins of diverse structural fabrics. Although both DSDP and ODP have targeted separate forearcs undergoing either tectonic erosion or accretion, Leg 112 was the first cruise to

investigate the Andean forearc, which, in the segment drilled, has been shown to have a history of both tectonic erosion and accretion during the late Neogene (Kulm et al., 1981; von Huene et al., 1985). The variety of tectonic environments encountered during Leg 112 drilling ranges from those characterized by extension and subsidence in the shelf and slope basins to compressional regimes of the accretionary complex.

This study documents the nature and range of occurrence of structural features encountered during Leg 112 drilling. Sediments indicating a wide range of environments, including shelf, upper, middle, and lower slope, were drilled. From these results a number of distinct tectonic provinces having characteristic structural styles can be delineated. Vein structures (which are discussed only briefly) are dealt with by companion studies in this volume (Lindsley-Griffin et al. and Kemp, this volume).

REGIONAL SETTING

Regional studies of the Andean continental margin undertaken during the Nazca Plate Project (Kulm et al., 1981) provided the framework upon which the tectonic objectives of Leg 112 were based. These studies show that the Peruvian forearc between 8° and 14°S is divided into five major basins: the Salaverry/East Pisco Basin, occupying the shelf, and the Trujillo, Yaquina, Lima and West Pisco basins along the continental slope (Thornburg and Kulm, 1981) (Fig. 1). The shelf and slope basins are separated by the outer shelf high—a submarine continuation of the Coast Range, which comprises Paleozoic metamorphics cut by Mesozoic igneous rocks.

The slope basins are bounded by the outer shelf high and the upper-slope ridge—another distinct and pivotal structural lineament. Results of Leg 112 drilling show that these basins had a complex and varied Cenozoic depositional history.

The presence of a narrow, frontal accretionary complex, inferred by previous studies, was confirmed by reprocessing of multichannel seismic (MCS) data (von Huene et al., 1985). The narrowness of this 15-km-wide zone of accretion, together with the tectono-stratigraphy of the forearc basins, confirms a history of alternating margin truncation (subduction erosion) and accretion for the sector.

¹ Suess, von Huene, et al., 1990. *Proc. ODP, Sci. Results*, College Station, TX (Ocean Drilling Program).

² Dept of Oceanography, Univ. of Southampton, Southampton, SO9 5NH, United Kingdom.

³ Dept of Geology, Univ. of Nebraska, 214 Bessey Hall, Lincoln, NE 68588-0340.

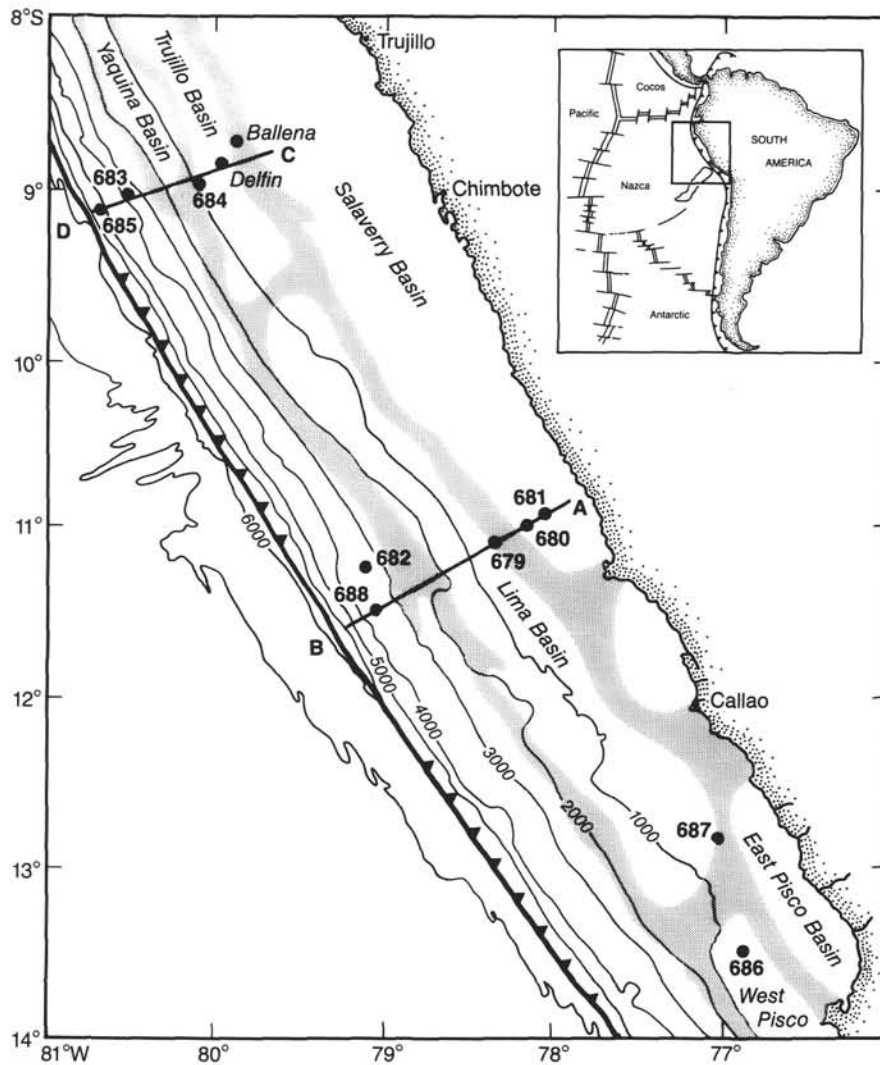


Figure 1. Map of the Peruvian continental margin, with bathymetric contours that show the location of Leg 112 drilling sites and seismic records CDP-1 (Line A-B) and CDP-2 (Line C-D).

Drilling during Leg 112 was concentrated along two cross-margin transects corresponding to the locations of two MCS reflection profiles (Figs. 1 through 3), with another two sites in the southern Lima and East Pisco basins. Sampling at these 10 sites revealed a comprehensively wide range of environments from the shelf and upper-slope through mid- and lower-slope basins, including the accretionary complex. The data presented below yield new information on the origins and variety of deformational styles represented at active margins.

STRUCTURAL FEATURES

Structural data were collected by shipboard sedimentologists from all the cores recovered and opened during Leg 112. A summary of the variation in occurrence of structural features is presented in Figure 4. In this summary, we attempted to conform as much as possible with the symbols of Lundberg and Moore (1986). Three major columns depict bedding orientation, pervasive fabrics, and discrete structures whose nature and occurrence are discussed in detail below. Details of lithologic unit and age are also given. Except for those in Unit IA of Site 685 and in Unit III of Site 688, bedding dips are mainly apparent dips. The absence of

bedding orientation data, such as for much of the Quaternary section of Site 688, results from a lack of marker surfaces (in this case, because of pervasive bioturbation). Lithologic variation is discussed briefly below, followed by descriptions of individual structural features and, because of its significance, a detailed account of the structural features encountered at Site 685.

Variations in Sediment Composition

Neogene lithologies recovered from the Peruvian margin are predominantly variably diatomaceous muds or mudstones (Figs. 2 and 3). The exception to this is the middle Miocene of Site 679, which consists of interbedded sandstones and shales. Thus, little compositional variation occurs in the Quaternary and Pliocene sections, other than the presence or absence of planar bedding anisotropies that result from diatom ooze laminae or sand and silt beds. Eocene lithologies encountered at Sites 688 and 682 comprise interbedded sandstones, calcareous sandstones, mudstones, and marls, and the thin Eocene section recovered from Site 683 is made up of mudstones. Variations in sediment composition are discussed in greater detail in Kemp and Hill (this volume).

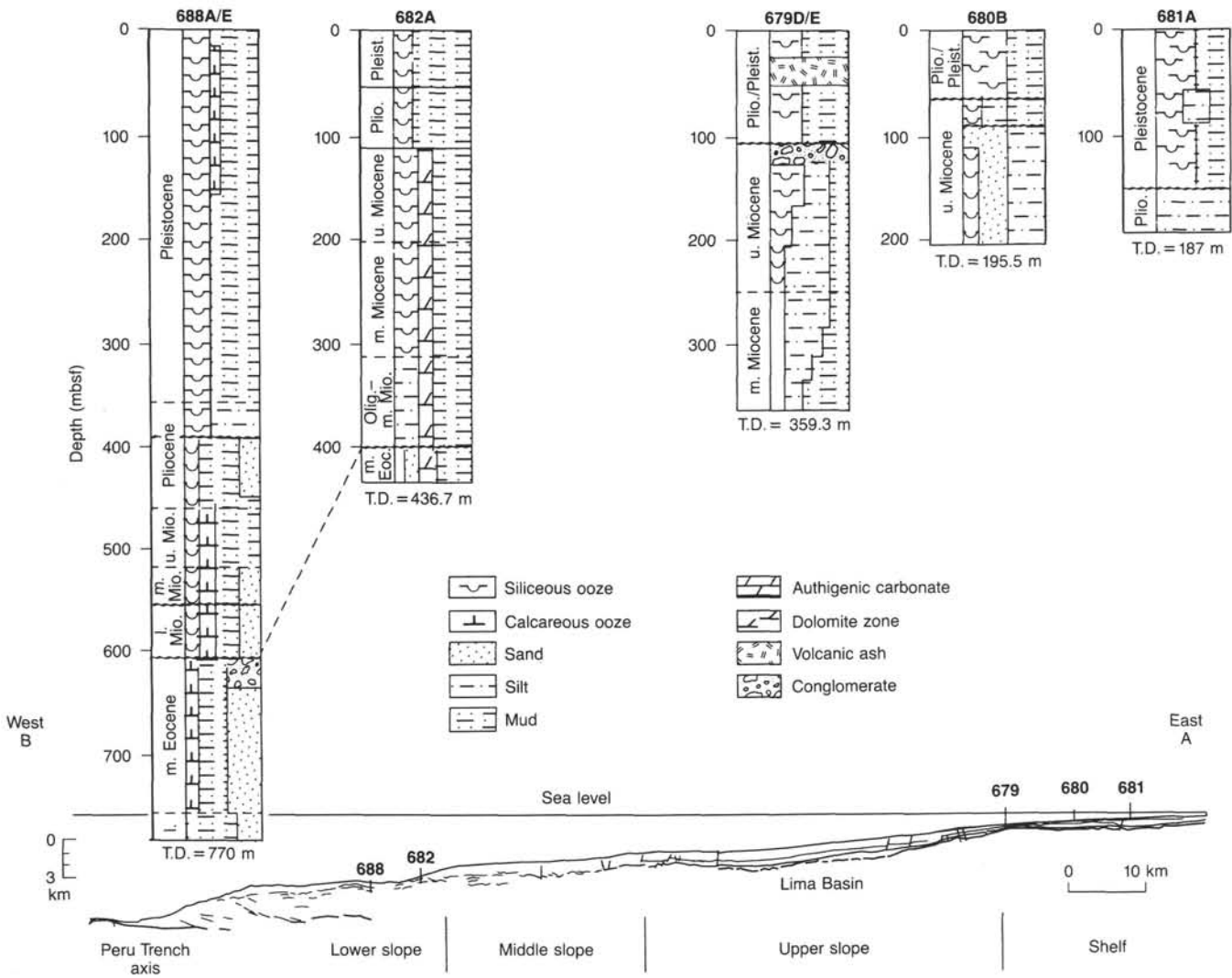


Figure 2. Trace of seismic record CDP-1, showing location of sites drilled along the southern transect (after von Huene et al., in press).

Bedding Orientation

Distinctive regional and stratigraphic patterns occur in the variation of bedding orientation (Fig. 4). Quaternary and Pliocene sediments recovered from the shelf and upper-slope basins (Sites 680, 681, 684, 686, and 687) have uniformly horizontal bedding, except for rare, thin, slumped intervals. Localized tilting of bedding at Site 679 probably relates to motion on an adjacent normal fault, identified from seismic records. In the southern transect, the Quaternary sediments recovered from the lower slope (Sites 682 and 688) appear to have horizontal dips (although much of the slope sequence is homogeneous and lacks evidence of bedding). The Pliocene and Miocene sediments (particularly from Site 688) have variable dips and exhibit other deformational features, which suggests slumping (see below). The Eocene section from Site 688 displays variable but generally moderate dips that may relate to tilting and locally observed folding.

Above the accretionary complex (Site 685), the upper part of the Quaternary slope sequence (Unit IA) displays horizontal bedding, with only localized tilting. The lower part of the slope sequence (Unit IB) has highly variable bedding orientation. The Miocene accretionary complex shows some variation, but mainly moderate dips of 30° to 50°.

Fissility

A more or less regular parting parallel to bedding that corresponds to fissility is developed in the deeper sections recovered from the continental slope (Sites 682, 683, 685, and 688). An incipient fissility is often developed from depths of 100 m and has been rarely observed as shallow as 35 m. However, a well-developed fissility is recognized only from depths of 250 m and below at Sites 682 and 683 and below 350 m at Site 688, which contains an expanded Quaternary section (Fig 4).

Scaly Foliation

The occurrence of scaly foliation is confined to the upper Miocene accretionary complex at Site 685 and the Eocene rocks of Sites 682 and 688. This structure, which is developed in mudstones, is composed of anastomosing curvilinear surfaces that may be polished and/or grooved. Most of the accreted sediments of Site 685 (Unit II) display a scaly foliation that is weakly to strongly developed (see below). The more mud-rich intervals of the Eocene sequence at Sites 682 and 688 display a scaly foliation that is associated with stratal disruption. Examination of this fabric using the shipboard scanning electron microscope showed it to be a microscopi-

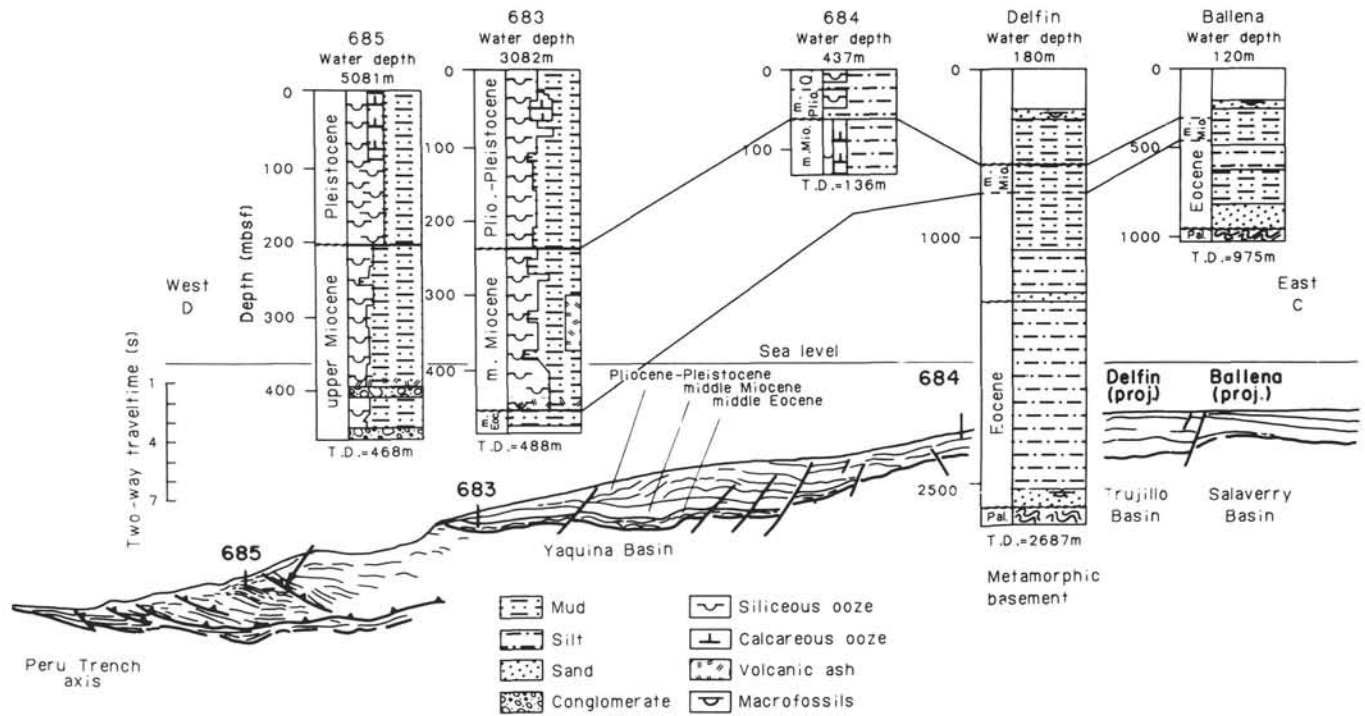


Figure 3. Trace of seismic record CDP-2 showing location of sites drilled along the northern transect (after von Huene et al., in press).

cally nonpenetrative, scaly foliation having discrete anastomosing polished movement surfaces separated by domains of undeformed mud (Pl. 2, Fig. 3). The identification of grooves on the polished surface supports evidence for displacement along this feature.

Vein Structures

Vein structures are primarily developed in the shelf and upper-slope basins (Sites 679 and 680, and to a lesser extent, Sites 681 and 686). The distribution and origins of these structures are discussed in detail in studies by Lindsley-Griffin et al. and Kemp (both this volume). These structures occur as *en-echelon* tension gashes, extensional (Pl. 1) microfaults, and larger discrete fissures and are often filled with fine material. Veins are most common at sites where normal faulting can be seen in seismic-reflection profiles. The distribution of these structures and recognition of analogous features in the Miocene Monterey Formation of California (Lindsley-Griffin et al., this volume) suggest that their occurrence is promoted by the effects of extensional tectonics on diatomaceous sediments.

Stratal Disruption

Zones of stratal disruption involving bedding discontinuities, microfaulting, and boudinage are developed extensively in three tectono-stratigraphic intervals: the upper Miocene of Site 685, the Eocene of Sites 682 and 688, and the Pliocene-Miocene of Sites 682 and 688. The stratal disruption at Site 685 is associated with a variably developed scaly foliation and is discussed in detail below.

In the Eocene sequence of Site 682, the scaly foliation described above is enhanced by a subparallel alignment of the long axes of elongate clasts of siltstone. Many of these clasts have elongated tails trailing off into the adjacent matrix and apparently have undergone boudinage by extreme necking. The sandy and silty lithologies generally occur as smeared out

blebs and pockets distributed in the matrix. Some boudinaged siltstone beds are barrel-shaped and display internal brittle fractures. This combination of brittle and ductile deformation suggests an early (pre-sand-cementation) onset for some of the deformation observed and that this occurred while there was little ductility contrast between sand and mud (although variations in pore pressure and strain rate may also have been significant). Similar deformational features occur in the more mud-rich intervals of the Eocene sequence at Site 688.

The Pliocene-Miocene section of Site 688 displays a wide range of stratal disruption associated with microfaulting and folding (Pl. 4, Figs. 1 through 3). The style of deformation varies according to lithology. Thick diatom-rich beds are dissected by networks of extensional microfaults and display incipient disintegration (Pl. 4, Fig. 1). Interbedded diatomite and mudstone show combinations of extensional microfaults and more ductile "necking" styles of boudinage. Locally, two phases of extensional deformation with low-angle bedding-subparallel faults cutting the early high-angle extension faults can be seen.

Folding

Folding was observed on a variety of scales from millimeter-scale in laminated intervals, to mesoscopic structures, to that inferred from variations in bedding orientation. Limited, generally intrafolial, minor folding occurs at several horizons in the upper-slope basins, where it is most probably related to minor slumping (Fig. 3). Intense, small-scale folding characterizes the finely laminated Pliocene-Miocene sequence of Sites 682 and 688, where it is closely associated with microfaulting and boudinage in more thickly bedded adjacent facies (Pl. 4, Fig. 3). In the lower part of the Quaternary at Site 685, highly variable bedding orientation suggests mesoscale folding (see below). Scattered bedding orientation in the Pliocene-Miocene section of Site 688 suggests that larger-scale fold structures may be associated with the minor fold observed at

this interval. Localized steep bedding in the Eocene sequence of Site 688 may also result from folding.

Faulting, Fracturing, and Brecciation

Extensive minor faulting in unlithified sediments is associated with vein structures and is referred to above. Fracturing was observed at several sites in rocks of upper Miocene age and older, and at depths greater than 200 m. Pervasive fracturing affected the Eocene of Site 683, the Miocene/Eocene boundary at Site 688, the Oligocene to middle Miocene of Site 682, and parts of the Miocene of Site 685. Considerable difficulties with hole conditions were encountered in all these sections, resulting in premature abandonment and, in the case of Site 682, requiring explosive decoupling.

In the Oligocene to middle Miocene (Unit III) of Site 682, much of the sediment within the drilling biscuits displays chaotic breccia fabrics. These fabrics are composed of subangular to rounded silty mudstone clasts in matrix support, grading to zones of interlocking angular to subangular clasts in framework support (Pl. 5, Fig. 2). Dimensions of the clasts vary from millimeters to centimeters. Breccia fabrics terminate at clearly defined biscuit boundaries, and the matrix is distinct from the drilling slurry in both color and consistency, thereby supporting a primary origin. At Site 688, the boundary between the Miocene and Eocene sequences is marked by a 30-m zone from which recovery was confined to only about 3 m of tectonic breccia that consisted primarily of calcareous and siliceous mudstone. Brecciation occurs at various scales and is locally gradational to thin zones of intense cataclasis. It seems probable that much of this interval is represented by cataclastic breccia, accounting for the poor recovery. The occurrence of sedimentary breccias and the intense fracturing that affects a substantial part of the upper Miocene in Unit IIB (Site 685) are discussed in detail below.

Discrete fractures are associated with the zones of brecciation described above and are frequently gradational to more pervasive brittle deformation. Elsewhere, fracturing is common in the middle-upper Miocene (Unit II) of Site 682, although a significant part of this might result from, or at least be accentuated by, drilling. The well-lithified, interbedded calcareous sandstones and marls of the Eocene section at Site 688 display a wide range of brittle deformation. This deformation ranges from numerous extensional microfaults, some with calcite vein infill, to developments of vein-filled fractures in massive sandstone. Brecciated and veined dolomites occur occasionally at several sites and are discussed in detail by Suess, Thornburg, et al. (this volume).

SITE 685: ACCRETIONARY COMPLEX AND SLOPE COVER

Slope Apron (Units IA, IB: 0–203.6 mbsf, Quaternary)

The sediments of the slope cover are composed of about 204 m of bioturbated diatomaceous muds interspersed with thin ooze and silt turbidities. From 0 to 74 mbsf (Unit IA), these sediments have horizontal dips and are undeformed. Only one interval (22–30 mbsf) shows gentle dips (5° – 25°) and is cut by small-scale normal faults (Pl. 1, Fig. 1). These faults have observed displacements of between 0.5 and 8 cm and generally have dips of between 30° and 80° , with a rare overturned fault set. These faults are also frequently infilled by thin (<mm) seams of dark bluish-black iron monosulfide and pyrite. Paleomagnetic orientation studies for this interval indicate that the beds are tilted and are downthrown toward the west (i.e., downslope).

From 74 to 203.6 mbsf (Unit IB), diatomaceous muds are extensively deformed. Measured bedding orientations are highly variable (Fig. 5) and include vertical dips at 123 and 129 mbsf, as well as local overturning (137 mbsf) that suggests mesoscale folding. Small-scale folding can be directly observed at 139 and 157 mbsf. An incipient fissility is developed from 75 mbsf and becomes stronger, although still sporadically developed, by 130 mbsf.

The boundary between Units IA and IB in Core 112-685A-9X at 74 mbsf coincides with the development of a planar fabric that cuts bedding at high angles. Plate 3, Figure 1, shows split halves of core viewed up hole. Section 112-685A-9X-2 (72 mbsf; Unit IA) displays a crude, coring-related radial fabric, but Section 112-685A-9X (78.5 mbsf; Unit IB) shows a planar fabric of uniform orientation that cuts the entire core. The fabric planes are discrete, polished surfaces having oriented grooves that exhibit subvertical displacement (Pl. 3, Fig. 2). Spacing of these fabric planes is typically between 0.5 and 3 mm at this level. This fabric increases in intensity downhole and becomes more closely spaced (Plate 3, Fig. 3), although still variable. Locally, thin (<0.1 mm) seams of fine-grained material occur within these fabric planes. Where the fabric is intense, it is locally anastomosing and resembles the more closely spaced mud-filled vein arrays of the upper-slope basin and shelf site (Pl. 1, Fig. 2), although it is pervasively developed at Site 685. Small offsets of bedding along fabric surfaces are common, providing further evidence for movement along fabric planes. These offsets resemble the microfaults observed in the shallower sites.

Orientation of the planar fabric varies, with dips typically ranging from 30° to 60° . However, this fabric appears everywhere to be perpendicular to bedding. In one observed example (Section 112-685A-10X-3; 84 mbsf), a fold in bedding also folds the fabric. Thus, the fabric appears (at least locally) to pre-date the folding of Unit IB. This distinctive planar fabric is present down to and including Core 112-685A-21X (194 mbsf). Cores 112-685A-19X through -22X (165.6–203.6 mbsf) exhibit partial induration, including both mud and mudstone. In Core 112-685A-22X (194.1–203.6 mbsf) an incipient scaly cleavage has developed.

Accretionary Complex (Units IIA, IIB: 203.6–383.1 mbsf, upper Miocene)

Nothing meaningful can be stated about observed deformation from 204 to 243 mbsf because of the minimal recovery of poor quality. From 234 to 271 mbsf, cores are highly brecciated by drilling, but sediment appears fragmented along a partly blocky parting transitional to a scaly foliation. This parting locally follows disrupted bedding. (See site chapters in *Initial Reports* of Leg 112 for discussion about the extent of drilling-related deformation.)

A pervasive scaly foliation is present from 272 mbsf and persists downcore, where its development is moderate to intense, with polished surfaces (Pl. 2, Fig. 2). This scaly foliation appears to be subparallel bedding, but where bedding/cleavage relationships can be clearly observed, the scaly foliation dips between 10° to 30° , shallower than bedding (at 290, 348 and 393 mbsf).

Well-preserved sections between 250 and 375 mbsf exhibit a range of brittle to ductile deformation, including microfaulting, boudinage, extreme necking, and disaggregation of beds to form clast-in-matrix textures that record the (mainly extensional) disruption of partially lithified sediment (Pl. 2, Fig. 1). Microfaults are closely spaced and although most are extensional faults, some thrust faults also occur. Brecciation and fracturing was only rarely observed in Unit IIA, but a striking example occurs at 385 mbsf, where a brecciated mudstone is

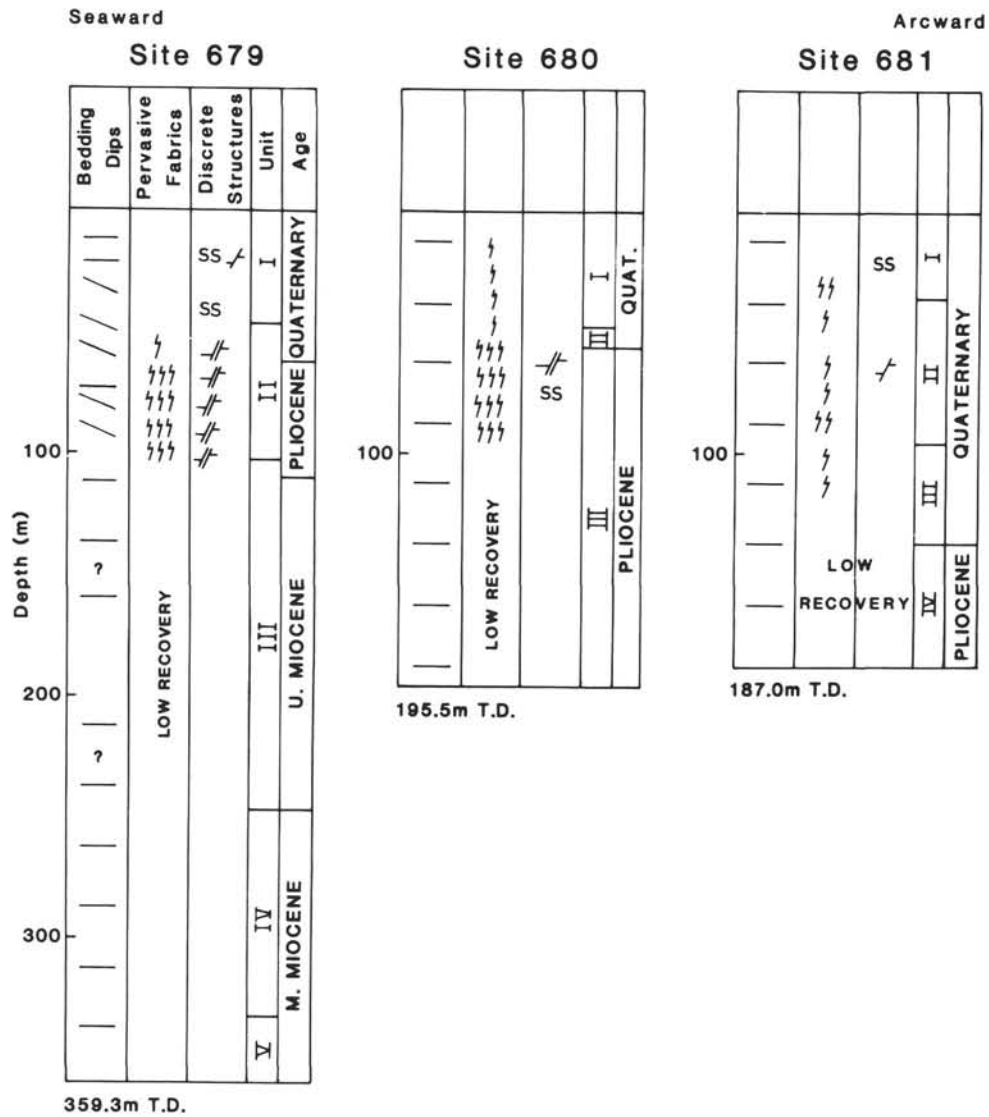


Figure 4. Synoptic structural logs of Sites 679, 680, 681, 682, 683, 685, and 688. Symbols mainly follow those of Moore (1986).

adjacent to a bed of intensely brecciated and veined dolomite (see Thornburg and Suess, this volume).

Primary sedimentary breccias occur in Unit IIB at two levels (402 and 459 mbsf; Pl. 5, Fig. 1). Clasts in these breccias include previously deformed diatomaceous mudstones of Eocene and lower Miocene age. Although these horizons are dominantly clast-supported, a crude scaly fabric is locally developed and more labile clasts are smeared out, subparallel to the scaly fabric.

A significant contrast in deformational style was observed below 402 mbsf (Unit IIB). An intense fracturing has developed, which is apparently superimposed on a scaly foliation (Pl. 5, Fig. 3). Three intersecting fracture planes are frequently present, in addition to the scaly foliation surfaces. Fracture planes are polished and grooved. Many of these surfaces exhibit compression normal to the core axis. One individual conjugate fault-pair was oriented paleomagnetically (Bourgeois and Langridge, 1988). A northeast-southwest axis of compression is indicated, assuming that the maximum compressive stress creates an angle of 30° with the two fault planes.

Interpretation of Structures at Site 685

The gentle oceanward dips and oceanward-facing normal faults of the upper part (Unit IA) of the Quaternary slope-apron sequence are consistent with gravitational processes operating on the slope. Disruption of bedding and folding within the lower part of the slope sequence (Unit IB) probably formed in response to downslope slumping. The high-angle fabric is transitional between the mud-filled microfaults and the *en-echelon* vein arrays of the upper-slope/shelf sites, but is more pervasively developed. The vein arrays and microfaults are fluid-escape conduits formed as the sediment underwent extension (Lindsley-Griffin et al. and Kemp, this volume). Generation of pervasive fluid-escape features also suggests that the deformation observed in Unit IB is related to downslope mass movement. Interestingly, the sediments of Unit IB contain abundant calcareous microfossils, in contrast to the overlying sediments, supporting a possible shallower water origin for the sediment of Unit IB with respect to the carbonate compensation depth (CCD).

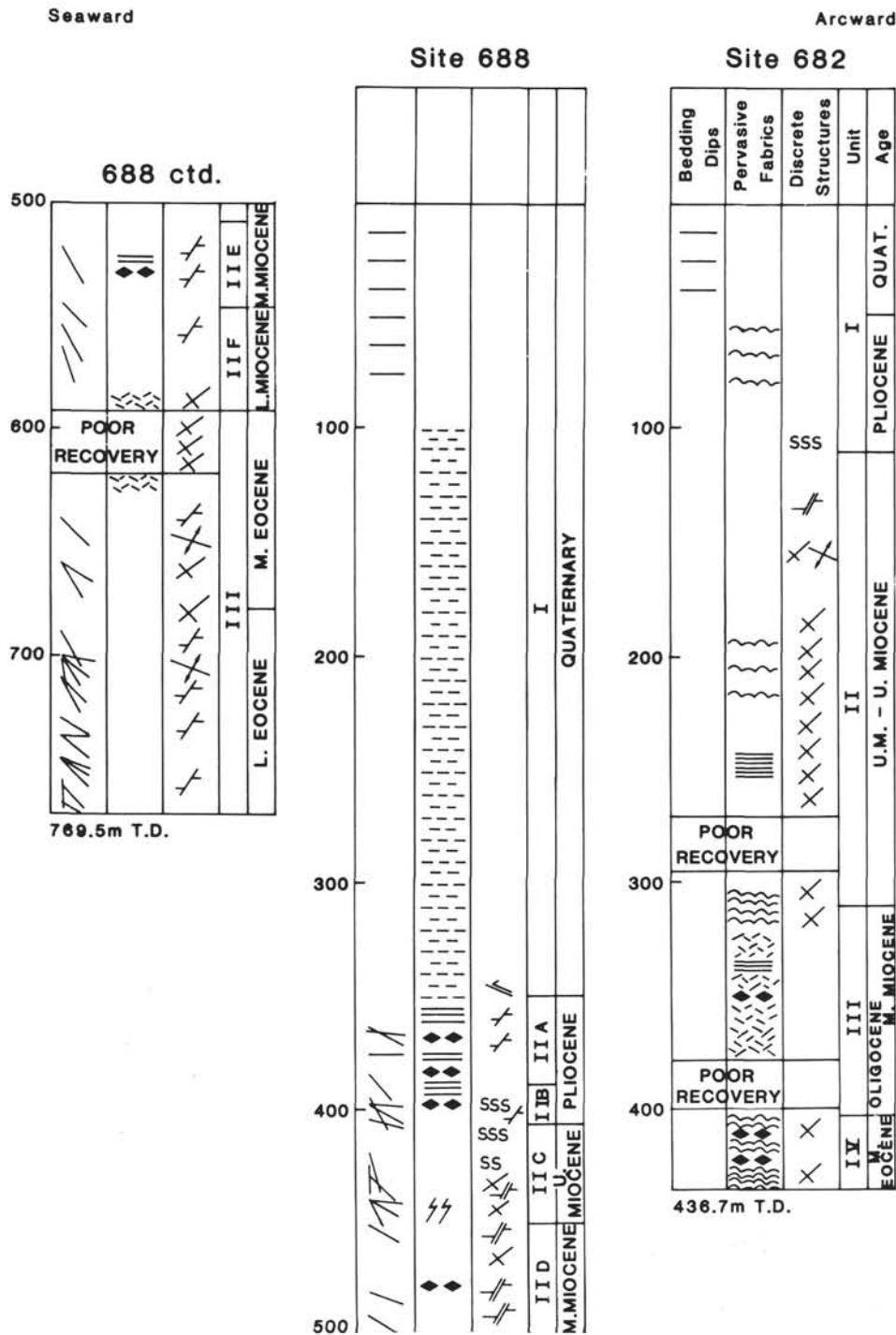


Figure 4 (continued).

The moderate-to-strong scaly foliation present in most of the accretionary complex (Unit II) of upper Miocene age marks a distinctive change in structural style from the overlying slope sediments and a contrast to deformation encountered on other slope sites. The development of this scaly foliation is consistent with underthrusting during accretion. The stratal disruption observed locally in Unit IIA may also relate to underthrusting, although there are more extensional, rather than compressional, features.

The intense fracturing in Unit IIB clearly is related to compression. The development of this fracturing coincides with an increase in carbonate content, as well as an increase in water content, with commensurate decrease in bulk density and increase in porosity. The higher water content and increased porosity may result from a fracture porosity induced in the sediment. This would account for the decrease in bulk density, which otherwise would be expected to increase during carbonate cementation. Alternatively, if the increased

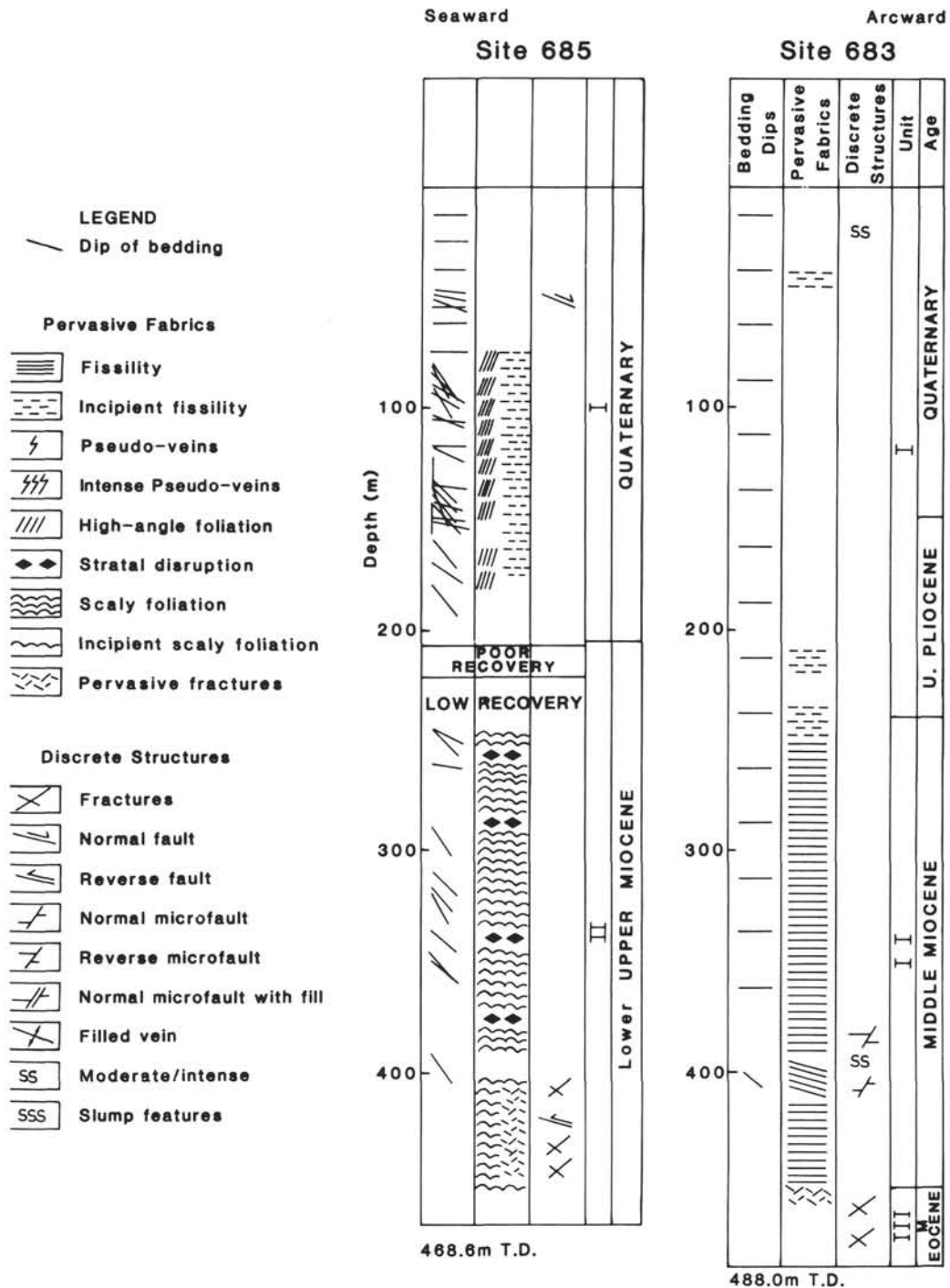


Figure 4 (continued).

porosity is integral to the rock, then the fracturing, coupled with the elevated water contents, might suggest hydraulic fracturing.

The bedding dips observed in Unit II are significantly higher than those estimated from the seismic-reflection profile. The surfaces imaged on the reflection record may represent faults. The steeper bedding orientation could then be explained by re-imbriication of the thrust stack. This might also account for the shallower dips of scaly foliation rather than bedding.

SUMMARY (VARIATIONS IN STRUCTURAL STYLE)

The range of structural features encountered during Leg 112 drilling occurs in distinct regional and stratigraphic patterns. These patterns delineate structural provinces having characteristic structural styles that reflect the complex tectonic history of the Peruvian forearc. Table 1 presents a synopsis of the structural features encountered at Site 685 and relates them to their environment of occurrence.

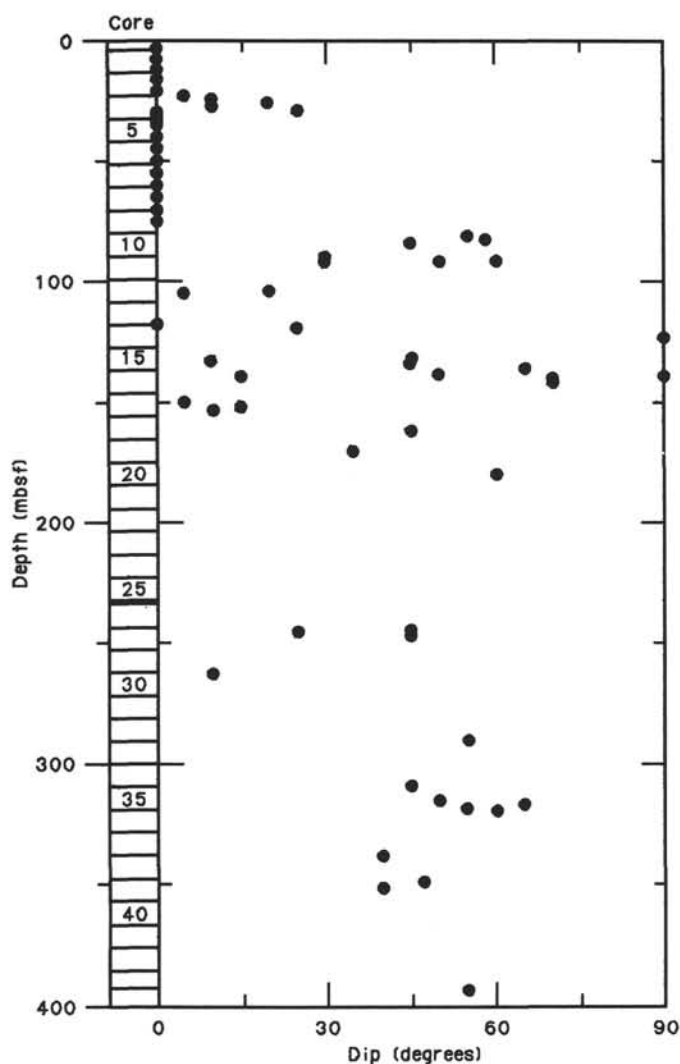


Figure 5. Dips of bedding at Site 685. Measurements in the top 200 m are true dips, measurements below are mainly apparent dips.

The Quaternary and Pliocene upwelling sediments of the Salaverry Basin (Sites 679, 680, and 681) contain vein arrays, extensional microfaults, and tension gashes, which are probably related to the combined effects of compaction, dewatering, and subsidence (see also Lindsley-Griffin et al. and Kemp, this volume). These structures are most intensely developed at Site 679, where bedding also is locally tilted. This site, located on the seaward margin of the Salaverry Basin, is adjacent to normal faults identified in seismic records. Thus, the development of vein structures may be promoted by an extensional tectonic regime.

The Quaternary sediments of the mid- and lower-slope sites (682, 683, 685, and 688) show few deformational features other than the ? slump-related deformation in the lower-slope sequence at Site 685. The development and recognition of structural features in these sediments is inhibited by their homogeneous texture, other than for thin turbidite beds.

The Pliocene through Miocene sequences of the slope Sites 682 and 688 and Pliocene through Eocene sequences of Site 683 are characterized by the presence of fissility and, at depth, by the development of locally intense fracturing, which was a serious obstacle to drilling. Localized evidence exists for

slumping at Sites 682 and 683. The entire 250-m Pliocene-Miocene section at Site 688 may represent a large slump or slide mass. Various forms of lithology-dependent deformation are present, including folding, mainly extensional (but also compressional) microfaulting, and disaggregation. Several biostratigraphic hiatuses in this sequence that coincide with zones of stratal disruption support evidence for slumping or sliding. Emplacement of this large slide mass may relate to the impingement on the margin of the Nazca Ridge in early Quaternary time (von Huene, Suess, et al., 1988).

The Eocene mudstones, siltstones, and sandstones encountered in the lower-slope Sites 682 and 688 exhibit a variety of structural features, including a scaly foliation, fracturing and veining, and some evidence for folding. This scaly foliation does not affect the overlying Miocene and (at Site 682) Oligocene slope sediments. Thus, the structures observed in the Eocene sequence probably formed in response to a late Eocene/Oligocene tectonic episode.

The sediments at Site 685 on the lower slope contain the clearest junction between slope cover and accretionary complex hitherto encountered during DSDP and ODP drilling. The upper part of the Quaternary slope cover is relatively undeformed, with only localized oceanward tilting and oceanward-facing normal faults. The lower part of the slope cover is folded and cut by a high-angle planar fabric, both probably related to slumping. The upper Miocene accretionary complex is characterized by moderate (45°) dips, the development of a scaly foliation, and locally intense, compression-related fracturing.

ACKNOWLEDGMENTS

We thank the Natural Environmental Research Council (UK) and National Science Foundation (USA) for supporting our participation in Leg 112. We thank our shipboard colleagues for their assistance in collecting data and for their stimulating discussion, especially Todd Thornburg, Jacques Bourgeois, Bob Langridge, and Roland von Huene.

REFERENCES

- COSOD II, 1987. Rept. 2nd Conf. on Scientific Drilling, Strasbourg, France.
- Kulm, L. D., Dymond, J., Dasch, E. J., and Hussong, D. M., 1981. Nazca Plate: crustal formation and Andean convergence. *Geol. Soc. Am. Mem.*, 154:824.
- Moore, J. C., 1986. Structural fabric in Deep Sea Drilling Project cores from forearcs. *Geol. Soc. Am. Mem.*, 166.
- Moore, J. C., Cowan, D. S., and Karig, D. E., 1985. Structural styles and deformational fabrics of accretionary complexes. Penrose Conf. Rept., *Geology*, 13:77-79.
- Suess, E., von Huene, R., et al., 1988. *Proc. ODP, Init. Repts.* 112: College Station, TX (Ocean Drilling Program).
- Thornburg, T., and Kulm, L. D., 1981. Sedimentary basins of the Peru continental margin: structure, stratigraphy, and Cenozoic tectonics from 6° to 16° latitude. *Geol. Soc. Am. Mem.*, 154:393-422.
- von Huene, R., Kulm, L. D., and Miller, J., 1985. Structure of the frontal part of the Andean convergent margin. *J. Geophys. Res.*, 90(B7):5429-5442.
- von Huene, R., Suess, E., and Leg 112 Shipboard Scientific Party, 1988. Results of Leg 112 drilling, Peru continental margin: Part I. Tectonic history. *Geology*, 16:934-938.

Date of initial receipt: 31 October 1988

Date of acceptance: 8 May 1989

Ms 112B-131

Table 1. Summary of deformational features at Site 685.

Lithologic unit	Core, section	Depth (mbsf)	Deformational features	Tectonic significance
IA	685A-1H-9X-3,	0-74	Localized, gentle oceanward-tilting of beds, oceanward-facing normal faults.	Gravity-related down slope extension.
IB	685A-9X-4 to 22X	80-203.6	Pervasive, high-angle planar, de-watering fabric and folding.	? downslope slumping and dewatering ? with a component of tectonic kneading.
II	685A-22X-51X	203.6-468.6	Scaly cleavage and localized compression-related fracturing. Rotation of bedding to moderate dips.	Thrusting during accretion.

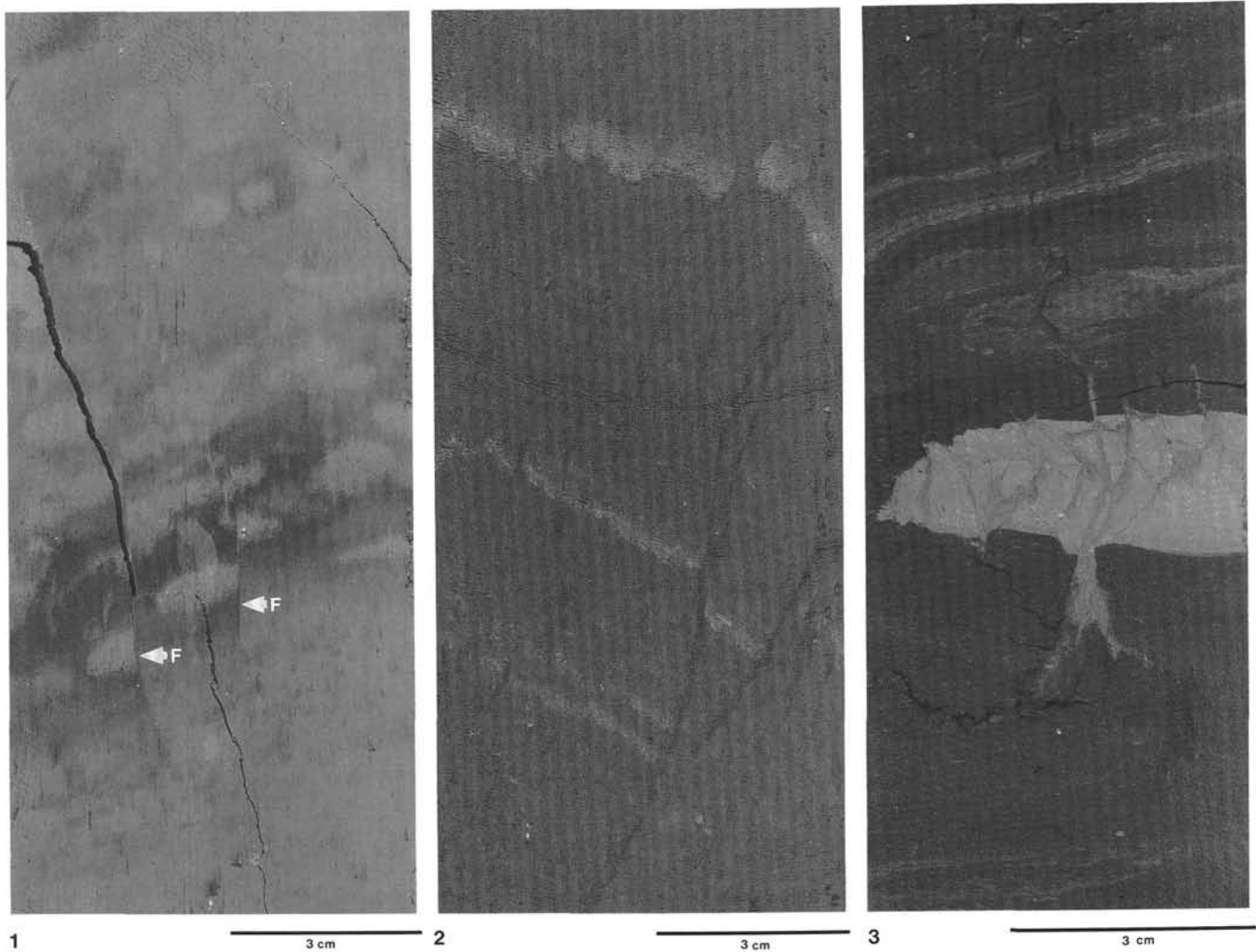


Plate 1. Examples of extensional faulting in outer-shelf and slope basins. **1.** Core photo of Sample 112-685A-4H-2, 60–73cm, foraminifer. Steep normal faults (marked F) cutting a bioturbated turbidite in the Quaternary slope cover at Site 685. Note also the dip of bedding oceanward (from right to left). **2.** Core photo of Sample 112-679B-8H-5, 44–58 cm. Complex, anastomosing extensional microfault pattern dissecting pale diatom ooze layers in diatomaceous mud of Pliocene age. Microfaults are infilled with fines from surrounding sediment (see papers by Kemp and Lindsley-Griffin et al., this volume). **3.** Core photo of Sample 112-679B-10H-7, 87–76 cm. Interbedded diatomaceous mud, diatom ooze laminae, and discontinuous dolomite bed in Pliocene age sediments. The partially cemented dolomite layer is dissected by extensional microfaults. Dolomite mud has been transported primarily downward, but also upward in associated fissures.

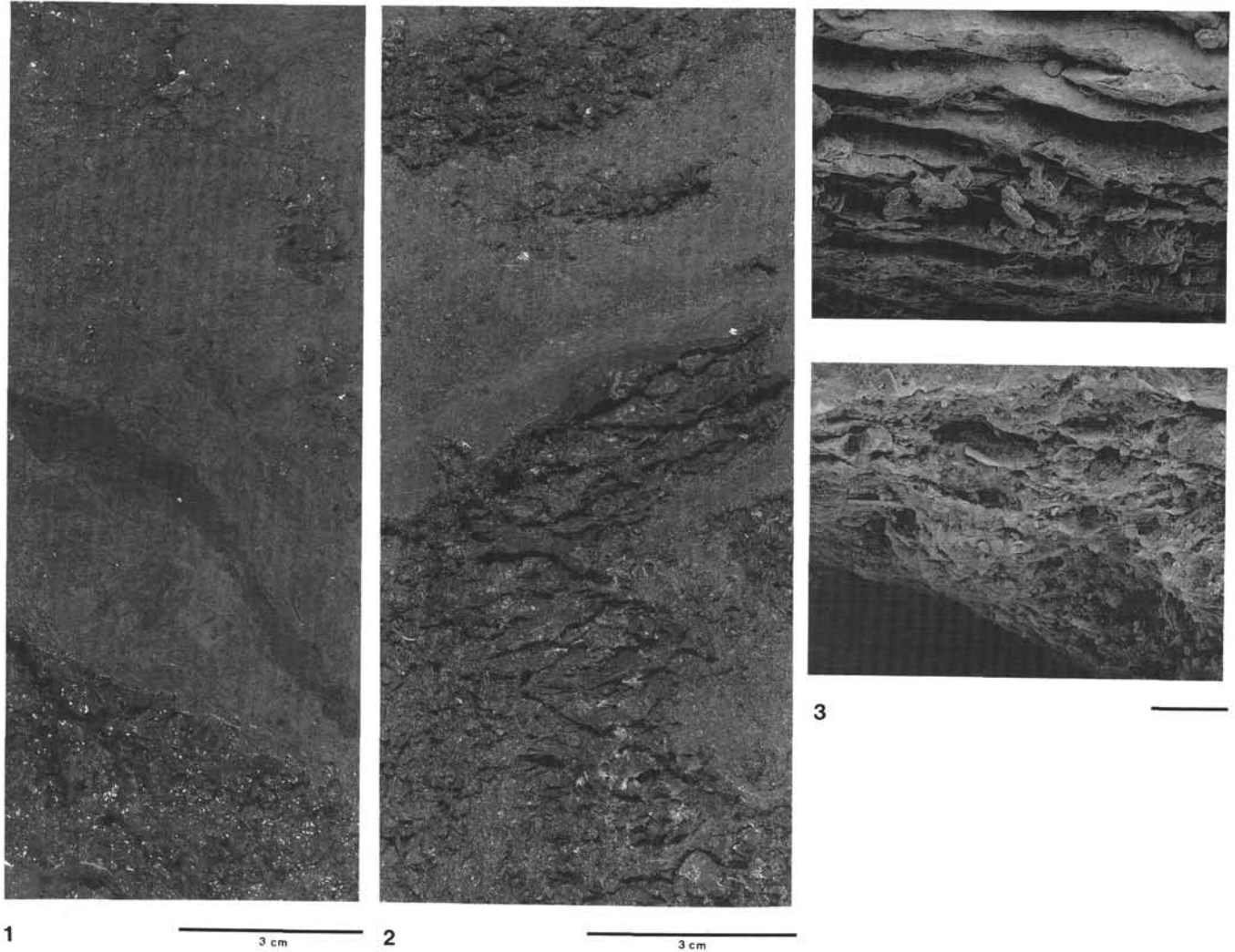


Plate 2. Scaly foliation and stratal disruption. **1.** Sample 112-685A-28X-2, 72–87 cm. Irregular pinch and swell of darker layer in upper Miocene accreted sediments showing typical (~45°) bedding dip and weak scaly foliation. **2.** Sample 112-685A-39x-3, 79–92 cm. Well-developed scaly foliation displaying polished surfaces in upper Miocene accreted sediments. The scaly foliation is subparallel to bedding. **3.** SEM photomicrographs of scaly foliation in Section 112-682A-46X-1; top = general morphology of scaly foliation encountered in the lower-slope Eocene section of Sites 682 and 688; bottom = detail of broken cleavage surface (top midright of upper photo), showing fabric as microscopically nonpenetrative.

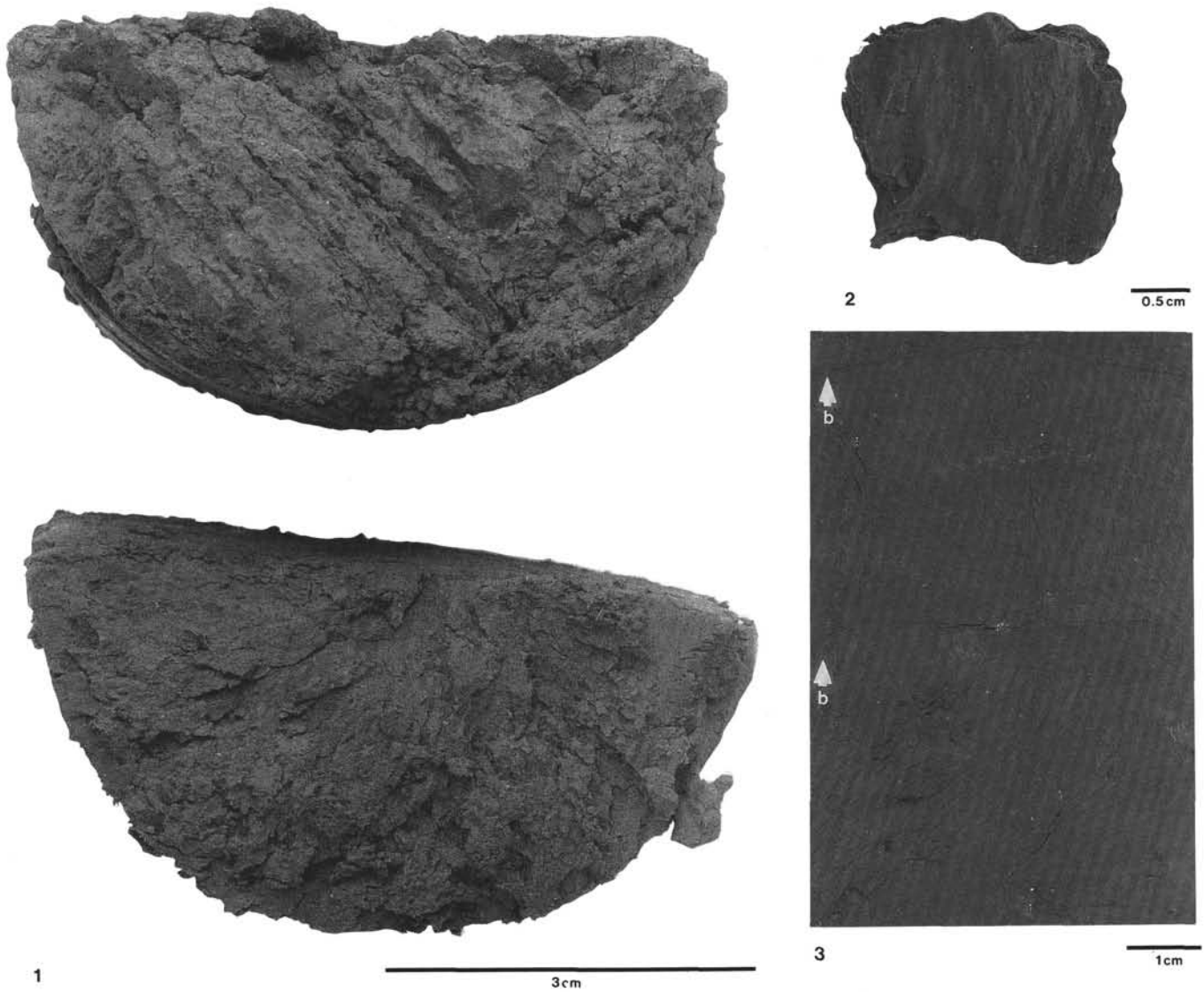


Plate 3. High-angle planar fabric in lower part of Quaternary slope cover in Hole 685A. 1. Split halves of Core 112-685A-9X (viewed uphole) showing (1) top-uniform planar fabric cutting core-surfaces dip steeply to lower left, Sample 112-685A-9X-2, 105 cm, Unit IA; (2) contrasted with bottom-crude, coring-related, radial fabric, Sample 112-685A-9X-8, 30 cm, Unit IB. 2. Sample 112-685A-9X-8, 7-8 cm. Detail of planar fabric of Figure 1 showing development of smooth, grooved planes evidencing motion along the fabric surfaces. 3. Sample 112-685A-10X-5, 76-84 cm. Cut surface of core showing dark traces of the high-angle planar fabric within biscuit boundaries marked (b). This core locally splits along the fabric, which is also seen to be anastomosing.

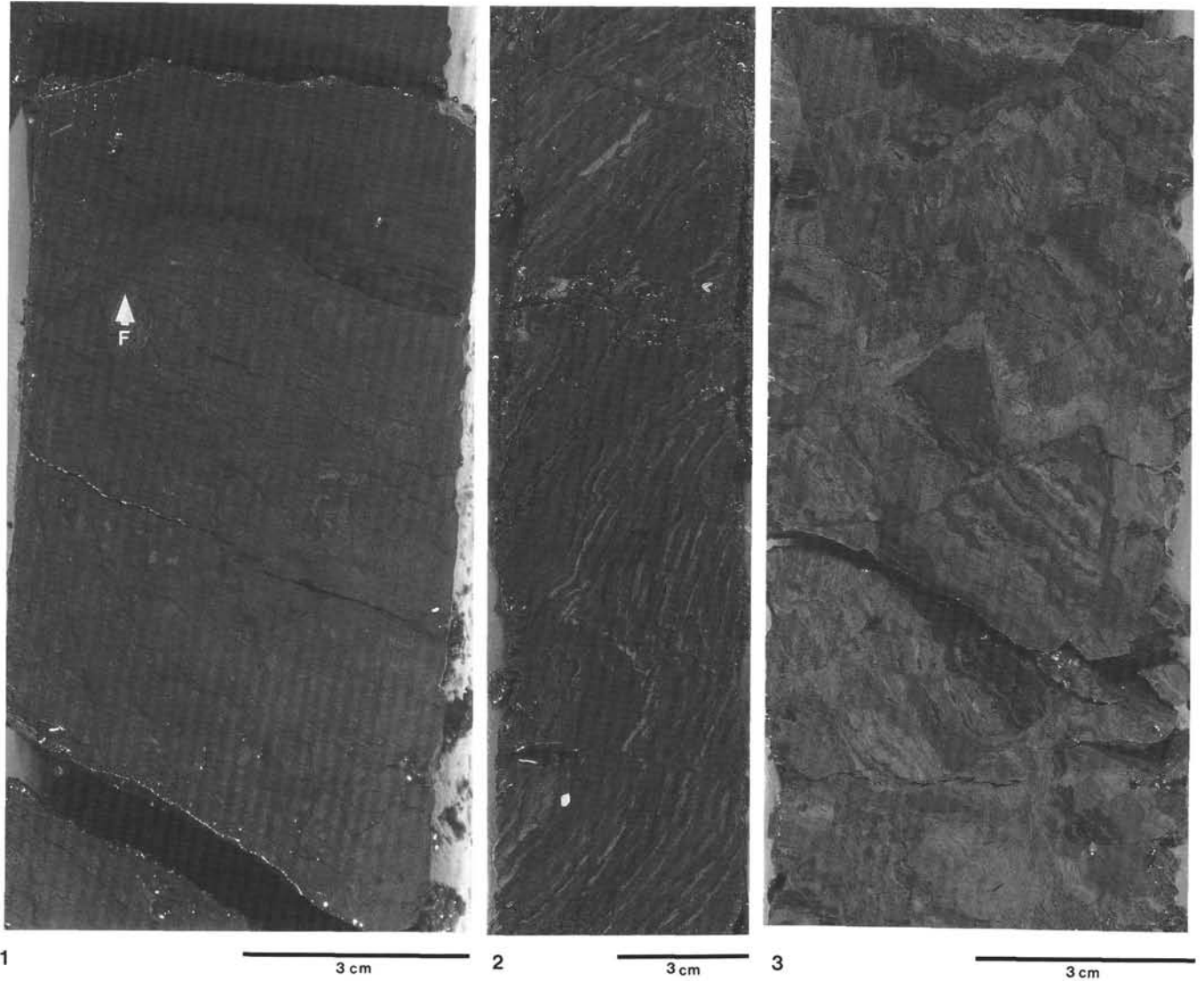


Plate 4. Varied extensional and compressional deformation structures characteristic of the 250-m-thick Pliocene-Miocene slope sequence (Unit II) from Site 688. **1.** Sample 112-688E-4R-1, 18–30 cm. Diatomaceous mudstone of Pliocene age, dissected by a network of fractures and faults, including prominent extensional fault in top (marked F). This has resulted in the effective *in-situ* disaggregation of the sediment. **2.** Sample 112-688E-6R-7, 8–30 cm. Diatomaceous mudstone with diatomite caminae of Pliocene-Miocene age that displays folding, with associated thrust microfaulting. **3.** Sample 112-688E-20R-1, 4–17 cm. Diatomaceous mudstone with diatomite laminae of middle Miocene age, dissected by complex networks of extensional microfaults of various scales. Some larger coherent fault-bound domains are surrounded by partly disaggregated sediment.

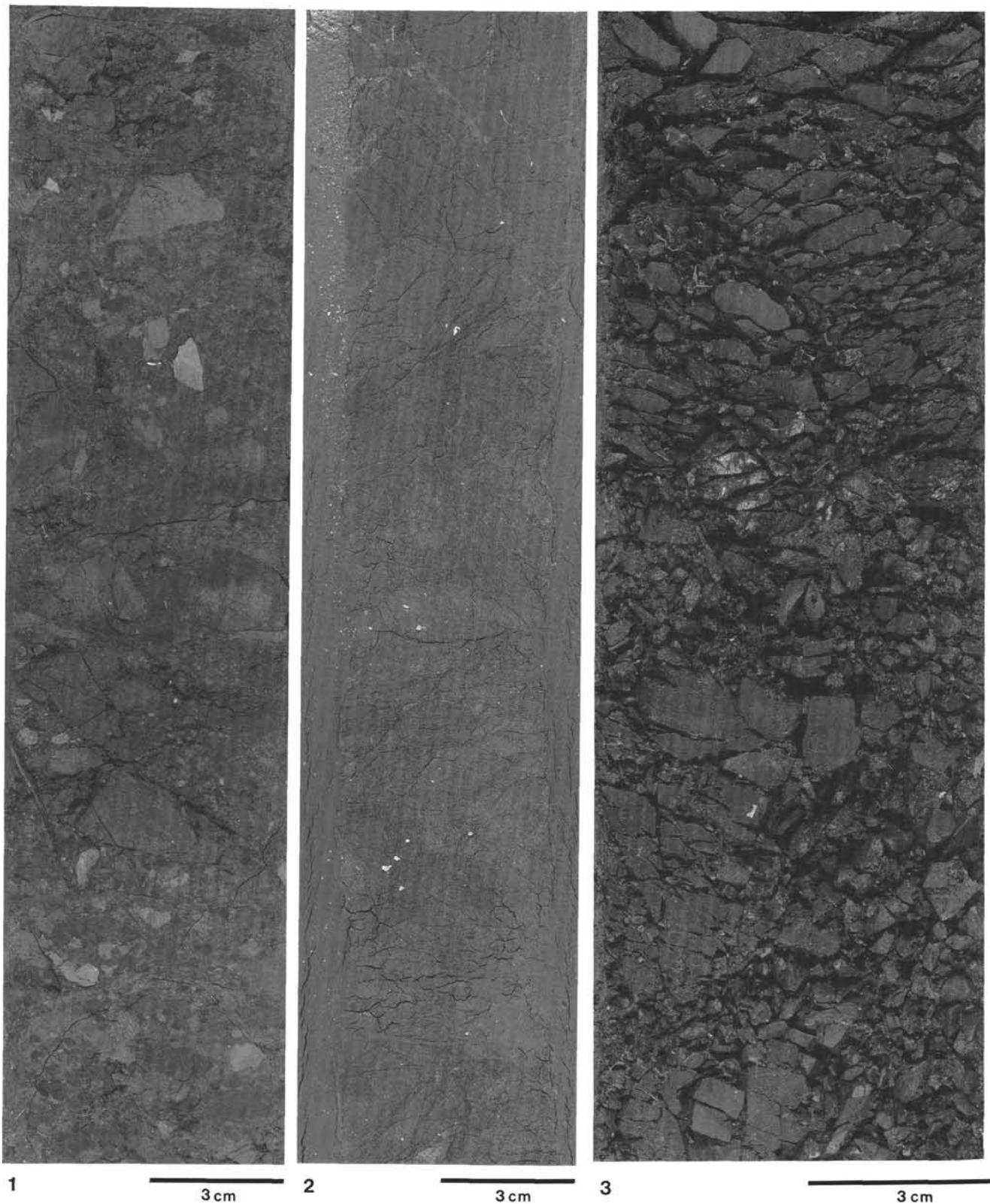


Plate 5. Examples of breccia fabrics from Leg 112 cores. 1. Sample 112-685A-44X-2, 118–144 cm. Sedimentary breccia of late Miocene age from the accretionary complex. The two breccia units recovered are clast-supported and contain a range of Eocene through Miocene clasts, some of which themselves display breccia fabrics. 2. Sample 112-682A-38X-3, 35–61 cm. Homogeneous diatomaceous mudstone of Oligocene-Miocene age displaying a network of fractures that result in a fabric of interlocking angular to subangular fragments. This represents *in-situ* fragmentation and is probably not drilling-related. 3. Sample 112-685A-48X-2, 16–34 cm. Intense conjugate fracturing developed in upper Miocene age diatomaceous mudstones of the accretionary complex. Note reflection on polished and grooved surface (center, and preexisting scaly cleavage, visible in the upper right).